14th July 2014

Nitrite/Nitrate Detection in Serum Based on Dual-Plate Generator-Collector Currents in a Microtrench

Andrew J. Gross [a*], Stephanie Holmes [a], Sara E. C. Dale [a], Miranda J. Smallwood [c], Stephen J. Green [b*], C. Peter Winlove [b], Nigel Benjamin [c], Paul G. Winyard [c] and Frank Marken [a]

[a] *Department of Chemistry, University of Bath, Bath, BA2 7AY, UK*

[b] *Department of Physics, College of Engineering, Mathematics and Physical Sciences, University of Exeter, Stocker Road, Exeter, EX4 4QL, UK*

[c] *University of Exeter Medical School, University of Exeter, St Luke's Campus, Exeter, EX1 2LU, UK*

To be submitted to Talanta

* Authors to whom correspondence should be addressed

Email: A.Gross@bath.ac.uk and S.J.Green@exeter.ac.uk

Abstract

A dual-electrode sensor is developed for rapid detection of nitrite/nitrate at micromolar levels in phosphate buffer media and in dilute horse serum without additional sample pre-treatment. A generator-collector configuration is employed so that on one electrode nitrate is reduced to nitrite and on the second electrode nitrite is oxidised back to nitrate. The resulting redox cycle gives rise to a specific and enhanced current signal which is exploited for sensitive and reliable measurement of nitrite/nitrate in the presence of oxygen.

The electrode design is based on a dual-plate microtrench (approximately 15 μm inter-electrode gap) fabricated from gold-coated glass and with a nano-silver catalyst for the reduction of nitrate. Fine tuning of the phosphate buffer pH is crucial for maximising collector current signals whilst minimising unwanted gold surface oxidation. A limit of detection of 24 μM nitrate and a linear concentration range of 200–1400 μM is reported for the microtrench sensor in phosphate buffer and dilute horse serum. Relative standard deviations for repeat measurements were in the range 1.8 % to 6.9 % (n = 3) indicating good repeatability in both aqueous and biological media. Preliminary method validation against the standard chemiluminescence method used in medical laboratories is reported for nitrate analysis in serum.

Keywords: nitrate, electrochemical sensor, electroanalysis, serum, bipotentiostat, microtrench,

1. Introduction

The construction of an electrochemical nitrate sensor that functions in the presence of oxygen in biological fluids with high selectivity against common background interferents such as cells, proteins and electrolytes, is highly desired for clinical studies and opens up the possibility of point-of-care assays for use in hospitals and healthcare settings [1, 2]. The use of electrochemical sensors is attractive as they are easily miniaturised, provide relatively quick results, are of good accuracy and are suitable for use in a wide range of solutions. These advantages can enable low level detection of analytes for clinical applications, as previously demonstrated by the success of electrochemical glucose biosensors [3].

Testing for the presence of nitrate in biological fluids such as serum has attracted increasing interest in recent years for clinical and sports science applications [4]. Nitrate levels produced endogenously represent the final product of nitric oxide (NO) and nitrite oxidation pathways, therefore providing an indication of NO levels and activity [4]. In clinical studies, nitrate levels have been used as a biomarker for potential diagnosis and monitoring of human health conditions such as infective and inflammatory diseases [5], cardiovascular [6] and neurological conditions [7]. Dietary or environmental exposure to nitrate has long been considered to be harmful due to risks associated with gastric cancer [8] and methemoglobinemia [9]. More recently, dietary nitrate supplementation has been shown to reduce blood pressure and lower the oxygen cost of sub-maximal exercise through enhancement of NO bioavailability [10-12].

Numerous methods have been established for detection of nitrate in aqueous and biological solutions including the Griess colorimetric assay [13, 14], fluorometric [15] and chemiluminescence [16, 17] methods, and methods based on solid-phase separation such as high-performance liquid chromatography [18], gas chromatography-mass spectrometry [14], ion chromatography [19] and capillary electrophoresis [20]. Whilst ion-selective electrodes are established for sensitive detection of nitrate in aqueous solutions [21], these electrodes are not used for nitrate analysis in biological fluids due to the presence of ionic interferents. The two best established methods for determining nitrate in biological fluids involve the reduction of nitrate to NO using vanadium (III) chloride, followed by either a relatively complex chemical test, the Griess reaction, coupled with colorimetric detection, or gas-phase chemiluminescent detection [13, 14, 17]. In general, these techniques provide very accurate results but require the use of specialist equipment, tedious procedures and take extended periods of time to perform. Furthermore, vanadium chloride and alternative reducing agents based on cadmium reagents are highly toxic. Nitrate reductase is also used as a reducing agent but requires careful handing in a controlled environment. Despite the wide range of methods available for nitrate detection in blood there is currently no rapid and convenient means of doing so for point-of-care testing.

Several electrochemical sensors and biosensors have been developed for detection of nitrate ions in aqueous solutions [22]. However, the electrochemical response is hindered by slow charge transfer kinetics leading to poor sensitivity and irreproducible measurements [22]. A wide range of electrode materials have been sought to combat this restriction including electrodeposited and bulk reactive metals

[23-26], chemically-modified electrodes with metal complexes [24], and composites based on silver graphite. Excellent limits of detection and good reproducibility have been reported in aqueous solutions but a lack of selectivity of bulk and chemically modified electrodes limits their applications in biological fluids [22]. Furthermore, the presence of dissolved oxygen impedes the reduction of nitrate and hence most electrochemical sensors to date require using degassed solutions. More sophisticated approaches have been developed based on the use of biological catalysts such as reductase enzymes which enable good sensitivity and impart a greater degree of selectively [27-29]. However, these bio-sensor systems suffer from the limitations of costly biological reagents, increasing complexity, and fragility of the electrode.

Small gap sensor electrodes operating in generator-collector mode via bipotentiostatic control are emerging as excellent candidates for sensing redox-active analytes at low concentrations [30]. Of particular interest are nano-gap electrodes [31-34], and simple low-cost microtrench electrodes developed recently in our laboratory [35-37]. The small spacing of these electrodes combined with the ability to control both electrode potentials independently provides access to enhanced current signals. Advantages included the ability to obtain amplified currents for a given molecule by redox-cycling ions between the two electrodes, access to steady state current responses free of capacitive current, and the ability to separate desired signals from interferents by elimination of chemically irreversible processes or by size-exclusion effects. To date, electroanalytical applications of generator-collector electrodes have been demonstrated for analytes including, for example, quinones [35, 37] and dopamine in the presence of known interferents [35].

In this work, we report the development of a silver-modified gold-gold microtrench electrode for nitrate detection which shows good sensitivity in generator-collector mode within a physiologically relevant concentration range (200 μM to 1400 μM). The proposed sensing mechanism is shown in Figure 1 (the redox system nitrite/nitrate is represented by Red/Ox). Within the microtrench, nitrate is converted by reduction to nitrite at one electrode (the "generator"), while nitrite is converted back to nitrate by oxidation at the other electrode (the "collector"). A repeating - and so signal-amplifying - redox cycle is achieved as these species interconvert and diffuse across the gap between the electrodes. After development of the electrode system in aqueous buffer, the analytical parameters of the electrode were investigated in horse serum diluted in phosphate buffer. The concentration of nitrate present in the samples was determined by the method of standard addition and compared against a standard gas-phase chemiluminescence method using a chemical analyser.

2. Experimental

2.1. Reagents

Potassium nitrate (KNO_3, ≥ 99 %), potassium nitrite (KNO_2, ≥ 96 %), silver nitrate ($AgNO_3$, ≥ 99 %), sodium hydroxide (98 %), potassium chloride (KCl, ≥ 99.0 %), monosodium phosphate monohydrate (98-102 %), disodium hydrogen phosphate heptahydrate (98-102 %), sulphuric acid (H_2SO_4, 95-98 %), hydrochloric acid (HCl, 37 %), nitric acid (HNO_3, 70 %), hydrogen peroxide (H_2O_2, 30 wt% in water) were all purchased from Sigma Aldrich, UK. Zinc sulphate, sodium nitrate (98+ %) and sodium iodide (99+ %) were purchased from Fisher. Vanadium (III) trichloride from Merck (99+ %) and glacial acetic acid (100 %) from VWR international. The serum

was prepared from fresh horse blood obtained from a local abattoir and stored in the freezer. Aqueous solutions were made with ultrapure water at 20 °C (resistivity ≥ 18.2 MΩ cm). Nitrogen (BOC) was employed for de-aerating solutions as required. Experiments were conducted at 20 ± 2 °C.

2.2. Instrumentation

Electrochemical measurements were obtained using either a CompactStat with bipotentiostat module (Ivium Technologies, Netherlands) with IviumSoft software 2.178 or a PGSTAT12 biopotentiostat system (Autolab, EcoChemie, Netherlands) with GPES 4.7 software. A conventional three or four-electrode cell was employed with a Pt wire counter electrode and saturated calomel electrode (SCE, Radiometer). The three electrode cell employed either a gold rod electrode ($\varnothing = 2$ mm) or one of the two electrodes of the microtrench. The four-electrode cell set-up employed the two working electrodes of the microtrench electrode.

Scanning electron microscopy (SEM) micrographs were recorded using a JSM-6480LV (JEOL, Japan). A 5 nm layer of chromium was sputter-coated onto the substrate prior to SEM analysis to remove charging and increase contrast.

Gas-phase chemiluminescent measurement of nitrate was performed using a Sievers Nitric Oxide Analyser (Sievers NOA 280i, Analytix Ltd, Durham, UK) [38, 39]. Prior to analysis, horse serum samples were thawed at room temperature then deproteinised using zinc sulphate precipitation. 200 µL of serum was added to 400 µL of 10% sodium hydroxide, followed by addition of 400 µL of 10% (w/v) zinc sulphate. The samples were thoroughly mixed using a vortex then allowed to react for 15 min. The

mixture was subsequently centrifuged and the supernatant analysed. The deproteinised samples were refluxed in 0.3 M sodium iodide and glacial acetic acid at 35 °C then analysed using the Nitric Oxide Analyser according to the methods described by Bateman and coworkers [38]. The nitrate concentrations of diluted serum samples were determined by the reduction to NO in a solution of 0.1 M vanadium (III) chloride in 1 M HCl at 95 °C. The gas-phase chemiluminescent reaction between NO and ozone was detected from the spectral emission of the electronically excited nitrogen dioxide product, using a thermoelectrically cooled, red-sensitive photomultiplier tube housed in the Sievers analyser. Calibration plots were obtained using standard sodium nitrate solutions.

2.3. Electrode Fabrication

Silver-gold microtrench electrodes were prepared from gold-gold microtrench electrodes fabricated using a method described previously [37]. Deposition of silver particles by chronoamperometry onto gold was employed here because silver is known to enhance the reduction of nitrate compared to bulk gold electrodes [40]. Gold-coated (100 nm) glass slides with a titanium adhesion layer were cut into 10 mm × 25 mm substrates then masked using Kapton tape (Farnell, UK) to give a masked strip in the centre of the electrode (≈ 5 mm × 25 mm). The exposed gold was then etched using aqua regia (1 : 3 v/v HNO_3 : HCl; **WARNING:** this solution is highly aggressive) for 3 min. After thorough rinsing of the samples in ultrapure water then drying with a stream of nitrogen, the Kapton tape was removed. The gold slides were heated at 500 °C for 30 min in the presence of air then cooled to room temperature. Two gold slides were placed on top of each other, with the gold surfaces face-to-face, and glued under pressure in a home-made press using epoxy (SP106 multi-purpose

epoxy, SP Gurit). After curing for 90 min, the end of the glued gold-gold electrode was sliced off using a diamond cutter and the new exposed surface polished using SiC paper (P320, Buehler). The epoxy layer between the gold-gold electrode was partially etched out by immersion in Piranha solution (1 : 5 H_2O_2 : H_2SO_4; **WARNING:** this solution is highly aggressive) for 3 min to yield the gold-gold microtrench electrode. It is noted that removal of the epoxy has no effect on the trench width. Silver was electrodeposited onto one of the gold electrodes by immersion of the polished end of the electrode into a solution of 1 mM $AgNO_3$ containing 0.1 M KNO_3. Using optimised chronoamperometry conditions, a fixed potential of -0.2 V *vs*. SCE was applied for 50 sec on the first working electrode. These parameters were chosen to facilitate the deposition of several layers of silver particles whilst minimising the possibility of a short-circuit between the two working electrodes. After deposition, the silver-gold microtrench was thoroughly rinsed with ultrapure water then dried with a stream of nitrogen prior to analysis. A silver-gold microtrench electrode was examined using SEM imaging (see Figure 1b) to confirm the gap size of approximately 15 μm. The microtrench electrodes can be used several times and were used for up to one week.

3. Results and Discussion

3.1. Dual-Plate Microtrench Electrode Preparation and Characterisation

The electrochemical responses of each of the gold electrode surfaces were first analysed in 0.1 M phosphate pH 5 to verify the successful fabrication of a clean gold-gold microtrench. Well-defined behaviour at positive potentials due to surface

oxidation and subsequent reduction of the gold oxide was observed at both electrodes (Figure 2a).

Deposition of the silver layer on the bare gold "generator" electrode was performed using chronoamperometry by applying a fixed potential of -0.2 V *vs.* SCE for 50 s in an unstirred 1 mM $AgNO_3$ solution with 0.1 M KNO_3 as supporting electrolyte. Supporting evidence confirming the presence of silver was obtained by cyclic voltammetry in phosphate buffer pH 5 (Figure 2b). The peaks are consistent with the successful deposition of silver on one of the electrodes [41].

3.2. Voltammetric Responses for Nitrite/Nitrate and Phosphate Buffer at Gold

The electrochemical oxidation of 10 mM KNO_2 in 0.1 M phosphate buffer solutions was initially examined using a gold electrode of the microtrench to observe the influence of solution pH on the electrochemical response of nitrite. The cyclic voltammograms obtained between pH 5 and pH 9 (Figure 3a) show that the peak current corresponding to nitrite oxidation (E_{pa} = 0.7 to 1.0 V *vs.* SCE) generally increases with decreasing pH whilst the peak potential shifts to less positive potentials with decreasing pH, consistent with previous studies [42]. As it has previously been observed that the oxide layer formed on gold electrodes hinders nitrite oxidation, experimental conditions were sought where oxide layer formation is minimised [43].

Figure 3b shows CVs obtained on the gold electrode in 0.1 M phosphate buffer (pH 5 to pH 9) solutions with no KNO_2 present. The well-known gold oxidation peak corresponding to surface oxide formation is observed on the forward sweeps in all cases and is found to shift to increasing potentials with increasing solution pH.

Greater stability towards gold surface oxidation is therefore obtained at more acidic potentials (Figure 3b, i). Based on the CVs recorded in Figure 3, the optimal pH for nitrite oxidation on the gold surface in the microtrench is pH 5. At this pH the overpotential required for nitrite oxidation is such that the rate of reaction is maximised and the influence of gold oxidation is minimised.

3.3. Voltammetric Responses for Nitrite/Nitrate at Gold/Silver Microtrench Electrodes: Potential Optimisation

The electrochemical reduction of nitrate ions is known to be a complex process in which nitrite, ammonia and nitrogen have been reported as bi-products depending on factors such as the electrode material, solution pH, and the electrode potential [23-25, 44, 45]. In neutral and acidic media (≥ pH 3), using metal-catalyst modified electrodes, it has been shown that reduction of nitrate yields nitrite as the main product via a two-electron process [23, 44]. Electrochemical oxidation of nitrite to nitrate via a multi-step two-electron process in neutral and acidic media (> pH 4) has been demonstrated on gold electrodes. On the basis of these studies, the proposed redox system exploited here for detection of nitrate using the microtrench electrode is shown in Equation 1.

$$NO_3^-(aq) + 2\,H^+ + 2\,e^- \rightleftharpoons NO_2^-(aq) + H_2O \qquad (1)$$

Detection of nitrate using the generator-collector approach is employed here by using the first working electrode ("the generator") to reduce nitrate to nitrite, and the second working electrode ("the collector") to oxidise nitrite back to nitrate. Figure 4a and 4b illustrate the electrochemical responses obtained using the silver-gold microtrench

electrode in 0.1 M phosphate buffer pH 5 solution before (i) and after (ii) addition of 10 mM KNO_3. In these experiments, the generator electrode was cycled between 0 V to -1.4 V *vs.* SCE, a potential range in which nitrate ions are known to be reduced, whilst the collector electrode was held at a fixed potential of 0.8 V *vs.* SCE, a potential sufficient to oxidise nitrite to nitrate (see Figure 3a). At the generator electrode (Figure 4a), the cyclic voltammograms reveal an increase in cathodic current in the potential range -0.6 V to -1.4 V *vs.* SCE following addition of KNO_3, consistent with electrochemical reduction of nitrate ions. A weak reduction peak observed at -0.2 V *vs.* SCE occurs due to oxygen reduction, and a well-defined reduction peak at -1.1V *vs.* SCE is attributed to reduction of the aqueous electrolyte solution (protons). At the collector electrode (Figure 4b), the electrochemical response observed in phosphate buffer without nitrate shows two characteristic peaks on the forward scan at -0.25 V and -1.25 V *vs.* SCE. The weak peak observed at -0.25 V *vs.* SCE is attributed to the two-electron oxidation of H_2O_2 which was generated by reduction of oxygen at ~ -0.2 V *vs.* SCE on the generator electrode. The peak at -1.25 V *vs.* SCE is attributed to processes associated with the electrolyte solution. On the collector electrode, following addition of 10 mM KNO_3 (Figure 4b, ii), a distinctly larger current signal which reaches a current plateau at -0.95 V *vs.* SCE is observed compared to the case with no nitrate present. The well-defined and expected limiting current plateau of the collector signal following addition of KNO_3 confirms the utility of the microtrench electrode to identify nitrate in a simple aqueous solution.

The interference of dissolved oxygen on the electrochemical reduction of nitrate is well-known, and as a result, electrochemical studies of nitrate reduction are typically performed in de-oxygenated solutions. Data obtained comparing the influence of

oxygen on the generator and collector current responses in 0.1 M phosphate buffer pH 5 containing 10 mM KNO_3 are shown in Figure 4c and 4d, respectively. The presence of oxygen was found to have little effect on the generator or collector response for nitrite/nitrate.

The effect of collector potential on the collector limiting currents was also investigated in phosphate buffer pH 5 containing 2 mM KNO_3. In these experiments, generator-collector voltammograms were obtained at 100 mV/s with the generator cycled between 0 to -1.4 V *vs.* SCE and the collector varied between -0.1 V and +0.9 V *vs.* SCE. A plot of the feedback currents as a function of collector potential is shown in Figure 5. The feedback currents were obtained by measuring the maximum current response at -0.95 V *vs.* SCE and subtracting these from the residual background current for each of the voltammograms recorded. As expected, the collector potential has a substantial effect on the observed feedback currents. At low potentials (-0.1 to +0.5 V *vs.* SCE) no current amplification effects are observed due to absence of redox-cycling of the nitrite/nitrate system between the generator and collector electrodes. When the collector potential is held at 0.6 V *vs.* SCE, a slightly larger current is observed compared to that observed between -0.1 to +0.5 V *vs.* SCE but a limiting current was not reached. At 0.6 V *vs.* SCE partial oxidation of nitrite is apparent and consequently a small amount of redox cycling takes place. Significantly larger feedback currents are observed when the collector potential is held in the range 0.7 to 0.9 V *vs.* SCE, with the highest feedback current observed at 0.8 V *vs.* SCE. At these potentials, the collector is set at or close to the redox potential of nitrite oxidation on gold (E_{pa} = 0.8 V *vs.* SCE, see Figure 3a) and hence nitrite ions are efficiently oxidised back to nitrate ions, resulting in large limiting feedback currents.

The slight drop in collector current observed when changing the collector potential from 0.8 V to 0.9 V *vs.* SCE is consistent with greater gold surface oxidation, which is known to hinder the nitrite oxidation process [43], therefore reducing redox-cycling efficiency. Data obtained at 100 mV/s gave the same optimised collector potential as was determined at slower scan rates (20 and 25 mV/s). The quality of the analytical signal was improved at slower scan rate and hence 25 mV/s was subsequently used for analytical determination of nitrate.

3.4. Electrochemical Determination of Nitrite/Nitrate at Gold/Silver Microtrench Electrodes: Phosphate Buffer Experiments

Figure 6a and 6b show generator and collector voltammograms recorded at 25 mV/s for the reduction of nitrate in 0.1 M phosphate buffer pH 5 in the (i) absence and (ii-viii) presence of KNO_3 at increasing concentrations in the range 200 μM to 1400 μM. Importantly, at this stage in the development of the microtrench sensor, an electrode pre-treatment step was introduced to minimise possible gold surface oxidation effects. The pre-treatment involved performing a generator-collector cyclic voltammogram with the collector held at 0.5 V *vs.* SCE (to initially reduce the collector electrode surface to gold metal). The pre-treatment was applied before recording each analytical voltammogram with the collector held at 0.8 V *vs.* SCE. The solution was agitated prior to recording each analytical voltammogram. At the generator electrode, very similar current responses were observed before and after addition of nitrate at various concentrations (Figure 6a). The generator current signal is therefore insensitive to nitrate addition. In contrast, at the collector electrode, a significant and systematic increase in current at ~ -0.95 V *vs.* SCE (limiting current plateau, see Figure 6b) was observed with increasing nitrate concentration. Simple measurement of the limiting

currents is possible due to the well-defined nature of both the current plateau and the residual background current. Additional peaks are observed at the collector electrode at -0.3 V and -1.2 V *vs.* SCE, tentatively assigned to the O_2/H_2O_2 and H^+/H_2 redox systems, respectively. These signals do not impact on measurement of the nitrate signal. The data in Figure 6b (inset) shows the blank subtracted calibration plot of collector feedback current as a function of KNO_3 concentration. A linear dependence of the collector current on concentration was observed over the concentration range tested with a coefficient of determination of 0.99, confirming that the microtrench sensor provides a suitable route for determination of nitrate concentration.

In order to test the method reproducibility several silver-gold microtrench electrodes was prepared and used for nitrate detection. Variability in collector current responses were observed due to variations in catalyst deposition and trench geometry. Typical analytical data are summarised in Table 1. Repeat measurements (n = 3) using one electrode were obtained in background electrolyte and for each of the calibration standards to test repeatability of the sensor. For the concentration range 100 μM to 1500 μM, the relative standard deviation (RSD) for the blank and each of the calibration standards was ≤ 3.9 %, demonstrating good within-run precision. Using the data in Table 1, the limit of detection (LOD), expressed as the analyte concentration corresponding to the blank mean value plus three standard deviations of the blank, was also determined. The estimated LOD using the method of standard addition in phosphate buffer is 5.3×10^{-7} A which corresponds to a standard concentration of 24 μM.

3.5. Voltammetric Responses for Nitrite/Nitrate at Gold/Silver Microtrench Electrodes: Serum Experiments

The feasibility of using the silver-gold microtrench electrode for application in biological fluids was investigated using horse serum. Prior to analysis, horse serum samples were thawed to room temperature then minimally diluted (1:1) in phosphate buffer pH 5, thoroughly mixed, then allowed to settle for 5 min. Figure 7 shows the generator and collector voltammograms obtained before and after addition of increasing amounts of potassium nitrate in the medically relevant concentration range 200 μM to 1400 μM. Concentrations between 4 and 45 μM are typical in human blood [46] but concentrations in patients with infectious medical conditions, for example, infective gastroenteritis, are known to increase to values in excess of 200 μM and as high as 1428 μM [5]. On the generator electrode, the current was found to increase but no systematic increase is discernible. On the collector electrode, surprisingly well-defined current responses were observed in serum before and after addition of nitrate (apart from a small shift in baseline), and importantly, were found to increase steadily with addition of aliquots of the same known concentration (200 μM). In comparison to the collector response obtained in phosphate buffer solution, a negative shift of 200 mV in the potential at which the limiting current is reached, is observed. The negative shift in potential observed in serum is, at least in part, attributed to adsorption of species such as proteins onto the electrocatalyst surface.

Figure 7b (inset) shows a standard calibration plot of collector feedback current as a function of KNO_3 concentration in unspiked diluted serum. A linear dependence of the collector current on concentration with $r^2 \geq 0.997$ is observed for both unspiked

serum and 500 μM spiked serum samples (where spiking of the sample from a stock solution of KNO_3 was undertaken prior to sample dilution).

Repeat measurements (n = 3) were obtained in background electrolyte and for calibration standards in the range 200 μM to 1400 μM to assess method precision. The RSD for the blank and each of the calibration standards ranged between 1.1 and 6.9 %, with greater precision being observed at the two highest concentrations. With the exception of the lowest calibration standard (200 μM), the relative standard deviations of < 5 % obtained show that the method exhibits a good level of reliability.

The KNO_3 concentration of the unspiked and spiked horse serum samples were obtained by extrapolation from the linear plots and determined to be 240 ± 10 μM (n = 2) and 781 μM, respectively (see Table 3). The spike recovery of 108 % is within 10 % of the expected spike value, providing evidence for good method accuracy. To assess the analytical performance of the method further, separate fractions of the same unspiked and spiked horse serum samples were analysed using a well-known routine chemical analyser method based on gas-phase chemiluminescence [38]. Unlike the electrochemical method which requires only minimal dilution of the serum, the chemical analyser method requires deproteinisation and five-fold dilution prior to analysis. Using the chemical analyser, the unspiked and spiked horse serum samples were determined to be 58 ± 10 μM (n = 2) and 539 μM, respectively (Table 3). These values are lower than those obtained using the electrochemical method and hence method bias arising from systematic error exists between the two methods. The discrepancy in concentrations between the two methods could potentially be

reconciled by a simple offset. Further study and improvement of the microtrench method will be required to resolve this problem.

4. Conclusions

It has been shown that generator-collector amplification for the nitrate-reduction / nitrite-oxidation redox cycle is possible with beneficial effects on the sensor current in a dual-plate gold/silver microtrench electrode system. Although sensitivity issues remain to be resolved, the major conclusions from this work are:

- Microtrench sensors can operate in the presence of dioxygen (no degassing required);
- Microtrench sensors function in serum-buffer media without further purification or separation;
- Microtrench sensors provide selectivity due to the use of two independently controlled electrodes set with different potentials (both generator and collector potential need to be correct to give the analytical response);
- Microtrench sensors can operate in the presence of low levels of interferences such as chloride or protein.

In future work, microtrench electrodes will be fabricated with a smaller inter-electrode gap using automated high-accuracy production techniques (e.g. photolithography) to significantly enhance sensitivity yet provide low-cost and reproducible sensor elements. Variation of the sensor catalyst and the type of electrode material should further widen the range of applications.

Acknowledgements

A.J.G. and F.M. gratefully acknowledge Higher Education Innovation Funding (HEIF) and the Engineering and Physical Sciences Research Council (EP/I028706/1) for financial support. S.J.G. acknowledges the University of Exeter for funding through the Higher Education Funding Council for England HEIF-5.

References

[1] Y. Wang, H. Xu, J. Zhang, G. Li, Electrochemical Sensors for Clinic Analysis, Sensors. 8 (2008) 2043-2081.

[2] A.I. Mian, M. Aranke, N.S. Bryan, Nitric oxide and its metabolites in the critical phase of illness: Rapid biomarkers in the making, Open Biochem J. 7 (2013) 24-32.

[3] J. Wang, Electrochemical glucose biosensors, Chem. Rev., 108 (2008) 814-825.

[4] G. Ellis, I. Adatia, M. Yazdanpanah, S.K. Makela, Nitrite and Nitrate Analyses: A Clinical Biochemistry Perspective, Clin. Biochem., 31 (1998) 195-220.

[5] R.S. Dykhuizen, J. Masson, G. McKnight, A.N.G. Mowat, C.C. Smith, L.M. Smith, N. Benjamin, Plasma nitrate concentration in infective gastroenteritis and inflammatory bowel disease, Gut. 39 (1996) 393-395.

[6] S.G. Ayub, T. Ayub, S.N. Khan, R. Dar, K.I. Andrabi, Reduced nitrate level in individuals with hypertension and diabetes, J Cardiovasc Dis Res. 2 (2011) 172-176.

[7] S. Milstien, N. Sakai, B.J. Brew, C. Krieger, J.H. Vickers, K. Saito, M.P. Heyes, Cerebrospinal fluid nitrite/nitrate levels in neurologic diseases, J. Neurochem., 63 (1994) 1178-1180.

[8] S.R. Tannenbaum, P. Correa, Nitrate and gastric cancer risks, Nature. 317 (1985) 675-676.

[9] F.R. Greer, M. Shannon, Infant methemoglobinemia: The role of dietary nitrate in food and water, Pediatrics. 116 (2005) 784-786.

[10] J. Kelly, J. Fulford, A. Vanhatalo, J.R. Blackwell, O. French, S.J. Bailey, M. Gilchrist, P.G. Winyard, A.M. Jones, Effects of short-term dietary nitrate supplementation on blood pressure, O2 uptake kinetics, and muscle and cognitive

function in older adults, Am. J. Physiol. Regul. Integr. Comp. Physiol., 304 (2013) R73-R83.

[11] A.M. Jones, S.J. Bailey, A. Vanhatalo, Dietary nitrate and O_2 consumption during exercise, Med. Sport Sci., 59 (2012) 29-35.

[12] S.K. Ferguson, D.M. Hirai, S.W. Copp, C.T. Holdsworth, J.D. Allen, A.M. Jones, T.I. Musch, D.C. Poole, Impact of dietary nitrate supplementation via beetroot juice on exercising muscle vascular control in rats, J. Physiol., 591 (2013) 547-557.

[13] I. Guevara, J. Iwanejko, A. Dembińska-Kieć, J. Pankiewicz, A. Wanat, P. Anna, I. Gołąbek, S. Bartuś, M. Malczewska-Malec, A. Szczudlik, Determination of nitrite/nitrate in human biological material by the simple Griess reaction, Clinica Chimica Acta. 274 (1998) 177-188.

[14] D. Tsikas, F.M. Gutzki, S. Rossa, H. Bauer, C. Neumann, K. Dockendorff, J. Sandmann, J.C. Frolich, Measurement of nitrite and nitrate in biological fluids by gas chromatography-mass spectrometry and by the Griess assay: problems with the Griess assay--solutions by gas chromatography-mass spectrometry, Anal. Biochem., 244 (1997) 208-220.

[15] A.K. Nussler, M. Glanemann, A. Schirmeier, L. Liu, N.C. Nussler, Fluorometric measurement of nitrite/nitrate by 2,3-diaminonaphthalene, Nat. Protocols. 1 (2006) 2223-2226.

[16] C.L. Walters, P.N. Gillatt, R.C. Palmer, P.L. Smith, A rapid method for the determination of nitrate and nitrite by chemiluminescence, Food Addit. Contam., 4 (1987) 133-140.

[17] A. Vanhatalo, J. Fulford, S.J. Bailey, J.R. Blackwell, P.G. Winyard, A.M. Jones, Dietary nitrate reduces muscle metabolic perturbation and improves exercise tolerance in hypoxia, J. Physiol., 589 (2011) 5517-5528.

[18] W.S. Jobgen, S.C. Jobgen, H. Li, C.J. Meininger, G. Wu, Analysis of nitrite and nitrate in biological samples using high-performance liquid chromatography, J. Chromatogr. B. 851 (2007) 71-82.

[19] J.M. Monaghan, K. Cook, D. Gara, D. Crowther, Determination of nitrite and nitrate in human serum, J. Chromatogr. A. 770 (1997) 143-149.

[20] P.N. Bories, E. Scherman, L. Dziedzic, Analysis of nitrite and nitrate in biological fluids by capillary electrophoresis, Clin. Biochem., 32 (1999) 9-14.

[21] P.J. Milham, A.S. Awad, R.E. Paull, J.H. Bull, Analysis of plants, soils and waters for nitrate by using an ion-selective electrode, Analyst. 95 (1970) 751-757.

[22] M.J. Moorcroft, J. Davis, R.G. Compton, Detection and determination of nitrate and nitrite: a review, Talanta. 54 (2001) 785-803.

[23] X. Xing, D.A. Scherson, C. Mak, Electrocatalytic reduction of nitrate mediated by underpotential-deposited cadmium on gold and silver electrodes in acid media, J. Electrochem. Soc., 137 (1990) 2166-2175.

[24] H.L. Li, J.Q. Chambers, D.T. Hobbs, Electroreduction of nitrate ions in concentrated sodium hydroxide solutions at lead, zinc, nickel and phthalocyanine-modified electrodes, J. Appl. Electrochem., 18 (1988) 454-458.

[25] G.E. Dima, A.C.A. De Vooys, M.T.M. Koper, Electrocatalytic reduction of nitrate at low concentration on coinage and transition-metal electrodes in acid solutions, J. Electroanal. Chem., 554-555 (2003) 15-23.

[26] M.-C. Tsai, D.-X. Zhuang, P.-Y. Chen, Electrodeposition of macroporous silver films from ionic liquids and assessment of these films in the electrocatalytic reduction of nitrate, Electrochim. Acta. 55 (2010) 1019-1027.

[27] T. Madasamy, M. Pandiaraj, A.K. Kanugula, S. Rajesh, K. Bhargava, N.K. Sethy, S. Kotamraju, C. Karunakaran, Gold nanoparticles with self-assembled cysteine monolayer coupled to nitrate reductase in polypyrrole matrix enhanced nitrate biosensor, Adv. Chem. Lett., 1 (2013) 2-9.

[28] T. Madasamy, M. Pandiaraj, M. Balamurugan, K. Bhargava, N.K. Sethy, C. Karunakaran, Copper, zinc superoxide dismutase and nitrate reductase coimmobilized bienzymatic biosensor for the simultaneous determination of nitrite and nitrate, Biosens. Bioelectron., 52 (2014) 209-215.

[29] D. Quan, J.H. Shim, J.D. Kim, H.S. Park, G.S. Cha, H. Nam, Electrochemical determination of nitrate with nitrate reductase-immobilized electrodes under ambient air, Anal. Chem., 77 (2005) 4467-4473.

[30] S.E.C. Dale, F. Marken, Electrochemistry within nanogaps in: J.D. Wadhawan, R.G. Compton (Eds.) Electrochemistry: Nanoelectrochemistry, RSC publishing, Cambridge, 2014, pp. 132-154.

[31] S.G. Lemay, S. Kang, K. Mathwig, P.S. Singh, Single-molecule electrochemistry: Present status and outlook, Acc. Chem. Res., 46 (2013) 369-377.

[32] M.A.G. Zevenbergen, P.S. Singh, E.D. Goluch, B.L. Wolfrum, S.G. Lemay, Stochastic sensing of single molecules in a nanofluidic electrochemical device, Nano Lett., 11 (2011) 2881-2886.

[33] S. Kang, A.F. Nieuwenhuis, K. Mathwig, D. Mampallil, S.G. Lemay, Electrochemical single-molecule detection in aqueous solution using self-aligned nanogap transducers, ACS Nano. 7 (2013) 10931-10937.

[34] A.T. Hubbard, D.G. Peters, Electrochemistry in thin layers of solution, Crit. Rev. Anal. Chem., 3 (1973) 201-242.

[35] M.A. Hasnat, A.J. Gross, S.E.C. Dale, E.O. Barnes, R.G. Compton, F. Marken, A dual-plate ITO-ITO generator-collector microtrench sensor: surface activation, spatial separation and suppression of irreversible oxygen and ascorbate interference, Analyst. 139 (2014) 569-575.

[36] S.E.C. Dale, F. Marken, Nano-litre proton/hydrogen titration in a dual-plate platinum-platinum generator-collector electrode micro-trench, Electrochim. Acta. 125 (2013) 94-100.

[37] S.E.C. Dale, F. Marken, Pulse electroanalysis at gold-gold micro-trench electrodes: Chemical signal filtering, Faraday Discuss., 164 (2013) 349-359.

[38] R.M. Bateman, C.G. Ellis, D.J. Freeman, Optimization of nitric oxide chemiluminescence operating conditions for measurement of plasma nitrite and nitrate, Clin. Chem., 48 (2002) 570-573.

[39] J. Kelly, J. Fulford, A. Vanhatalo, J.R. Blackwell, O. French, S.J. Bailey, M. Gilchrist, P.G. Winyard, A.M. Jones, Effects of short-term dietary nitrate supplementation on blood pressure, O_2 uptake kinetics, and muscle and cognitive function in older adults, Am. J. Physiol. Regul. Integr. Comp. Physiol., 304 (2013) R73-R83.

[40] K. Fajerwerg, V. Ynam, B. Chaudret, V. Garçon, D. Thouron, M. Comtat, An original nitrate sensor based on silver nanoparticles electrodeposited on a gold electrode, Electrochem. Comm., 12 (2010) 1439-1441.

[41] B. Habibi, M. Jahanbakhshi, M. Pournaghi-Azar, Voltammetric and amperometric determination of hydrogen peroxide using a carbon-ceramic electrode modified with a nanohybrid composite made from single-walled carbon nanotubes and silver nanoparticles, Microchim. Acta., 177 (2012) 185-193.

[42] Y. Wang, E. Laborda, R.G. Compton, Electrochemical oxidation of nitrite: Kinetic, mechanistic and analytical study by square wave voltammetry, J. Electroanal. Chem., 670 (2012) 56-61.

[43] B. Piela, P.K. Wrona, Oxidation of nitrites on solid electrodes I. Determination of the reaction mechanism on the pure electrode surface, J. Electrochem. Soc., 149 (2002) E55-E63.

[44] M.R. Majidi, K. Asadpour-Zeynali, B. Hafezi, Fabrication of Nanostructured Copper Thin Films at Disposable Pencil Graphite Electrode and its Application to Elecrocatalytic Reduction of Nitrate, Int. J. Electrochem. Sci. 6 (2011) 162-170.

[45] O. Ghodbane, M. Sarrazin, L. Roué, D. Bélanger, Electrochemical reduction of nitrate on pyrolytic graphite-supported Cu and Pd-Cu electrocatalysts, J. Electrochem. Soc., 155 (2008) F117-F123.

[46] H. Moshage, B. Kok, J.R. Huizenga, P.L. Jansen, Nitrite and nitrate determinations in plasma: A critical evaluation, Clin. Chem., 41 (1995) 892-896.

Figure Captions

Fig. 1 (a) Schematic drawing of the nitrate sensing mechanism by coupled nitrate reduction and nitrite oxidation. (b) Scanning electron microscopy (SEM) micrograph of the microtrench

Fig. 2 (a) Cyclic voltammograms (CVs) obtained at a gold-gold microtrench (i) generator and (ii) collector in 0.1 M phosphate buffer pH 5. (b) CVs obtained at the microtrench (i) collector and (ii) generator electrodes after silver deposition. Scan rate = 20 mV/s

Fig. 3 (a, b) CVs of a gold microtrench working electrode in 0.1 M phosphate buffer (a) containing 10 mM KNO_2 and (b) with no KNO_2 added at (i) pH 5, (ii) pH 6, (iii) pH 7, (iv) pH 8, and (v) pH 9. Vertical dashed lines at 0.75 V and 1.0 V *vs.* SCE indicate the nitrite and gold surface oxidation peak positions at pH 5, respectively. Scan rate = 20 mV/s

Fig. 4 (a) Generator and (b) collector voltammograms obtained at a silver-gold microtrench in 0.1 M phosphate buffer pH 5 (i) before and (ii) after addition of 10 mM KNO_3. (c) Generator and (d) collector signals obtained at a silver-gold microtrench (i) before and (ii) after removal of oxygen by nitrogen degassing for 10 min. Scan rate = 25 mV/s. Collector potential = 0.8 V *vs.* SCE

Fig. 5 Plot of the collector feedback currents as a function of collector potential in 0.1 M phosphate buffer pH 5 + 2 mM KNO_3. Scan rate = 100 mV/s

Fig. 6 (a) Generator and (b) collector voltammograms obtained at a silver-gold microtrench in 0.1 M phosphate buffer pH 5 (i) before and (ii-viii) after addition of KNO_3: (ii) 200 µM, (iii) 400 µM, (iv) 600 µM, (v) 800 µM, (vi) 1000 µM, (vii) 1200 µM, (viii) 1400 µM. Scan rate = 25 mV/s. Collector potential = 0.8 V *vs.* SCE. Inset shows plot of the collector feedback limiting currents versus KNO_3 concentration with background subtraction (line of best fit forced through zero)

Fig. 7 (a) Generator and (b) collector voltammograms obtained at a silver-gold microtrench in horse serum diluted 1:1 in 0.1 M phosphate buffer pH 5 (i) before and (ii-viii) after addition of KNO_3: (ii) 200 µM, (iii) 400 µM, (iv) 600 µM, (v) 800 µM, (vi) 1000 µM, (vii) 1200 µM, (viii) 1400 µM. Scan rate = 25 mV/s. Collector potential = 0.8 V *vs.* SCE. Inset shows plot of the collector feedback limiting currents versus KNO_3 concentration. Error bars correspond to one standard deviation of the mean

Table Captions

Table 1. Repeatability testing data using a silver-gold microtrench electrode for nitrate detection in 0.1 M phosphate buffer pH 5 using the method of standard addition

Table 2. Repeatability testing data using a silver-gold microtrench electrode for nitrate detection in horse serum samples diluted 1:1 in 0.1 M phosphate buffer pH 5 using the method of standard addition

Table 3. Summary of estimated nitrate concentrations obtained by redox-cycling using microtrench electrodes and by chemical analysis using the chemical analyser method

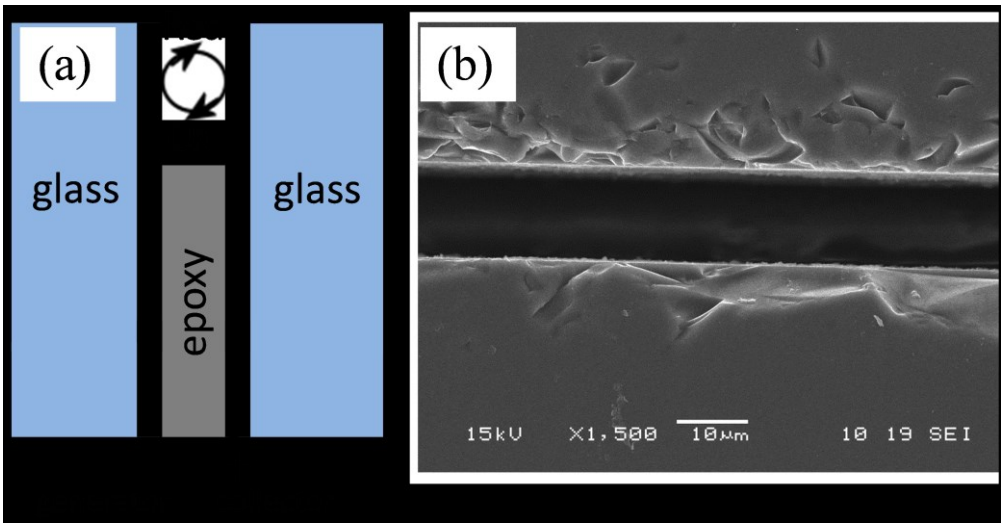

Figure 1

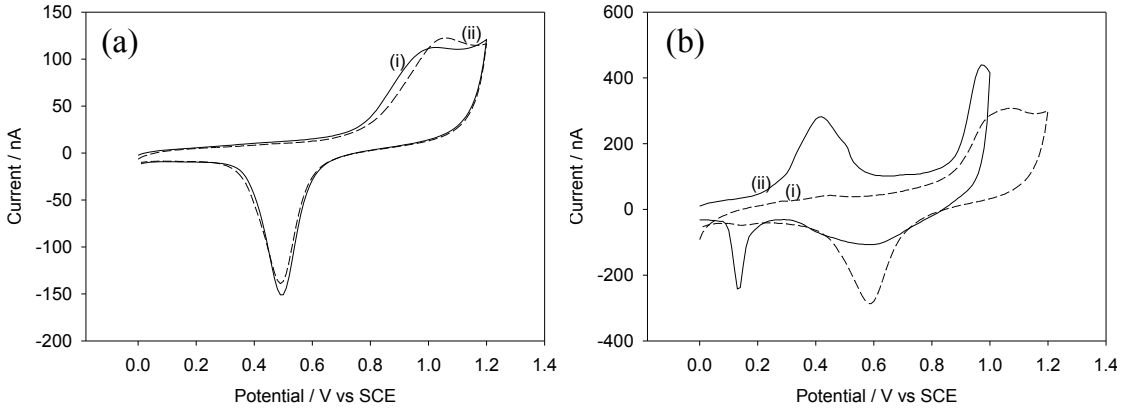

Figure 2

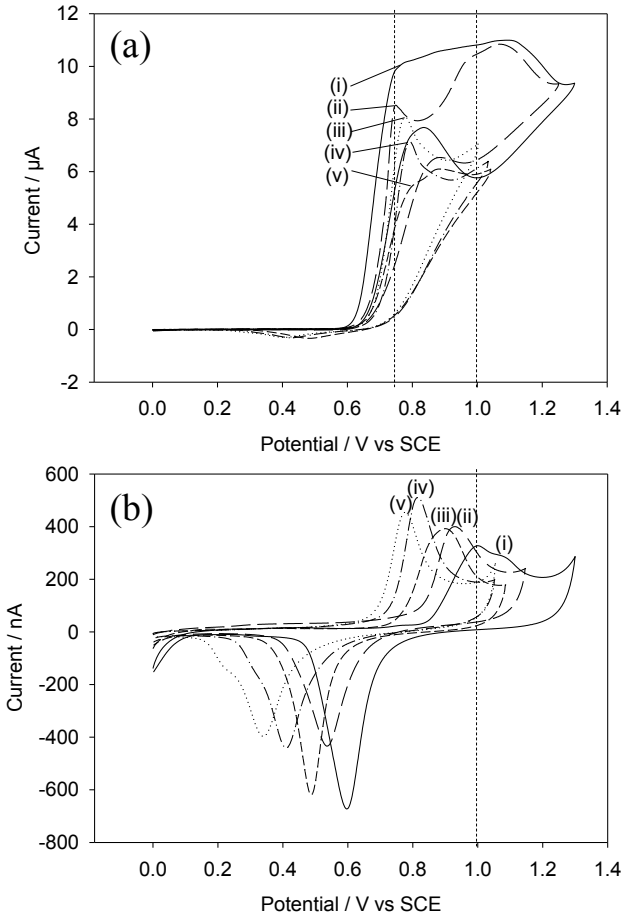
(a)
(i)
(ii)
(iii)
(iv)
(v)
Current / µA
Potential / V vs SCE
(b)
(iv)
(v)
(iii)(ii)
(i)
Current / nA
Potential / V vs SCE

Figure 3

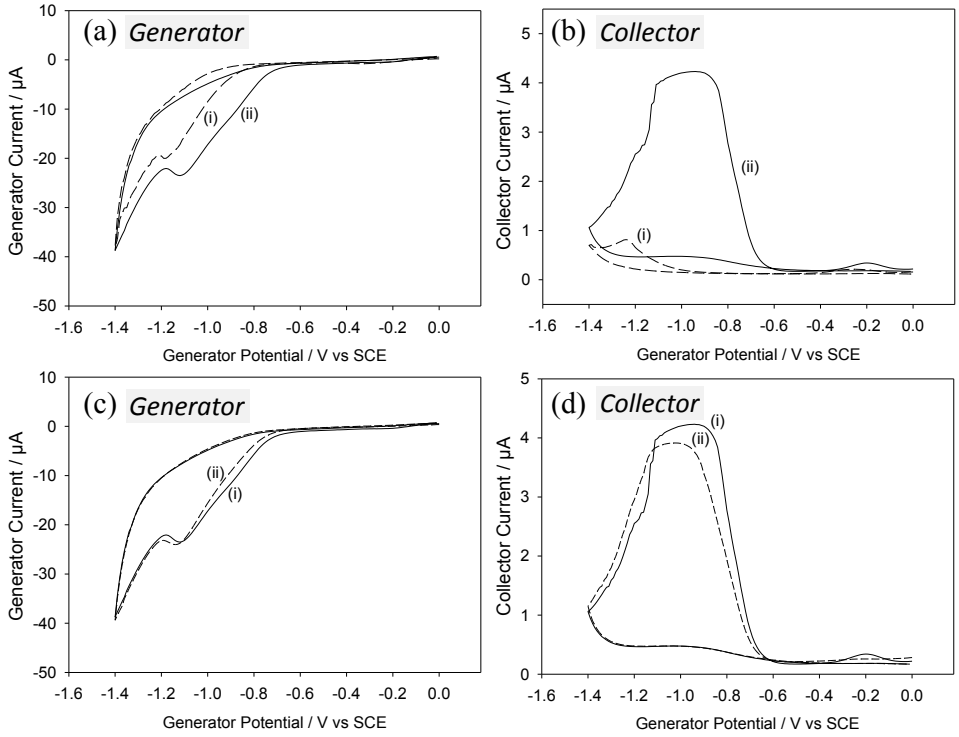

Figure 4

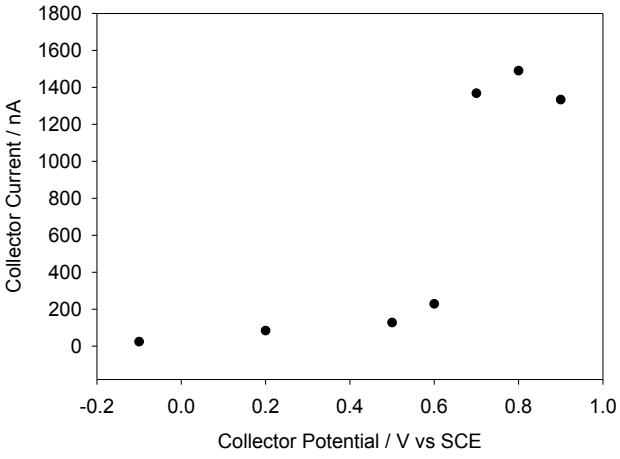

Figure 5

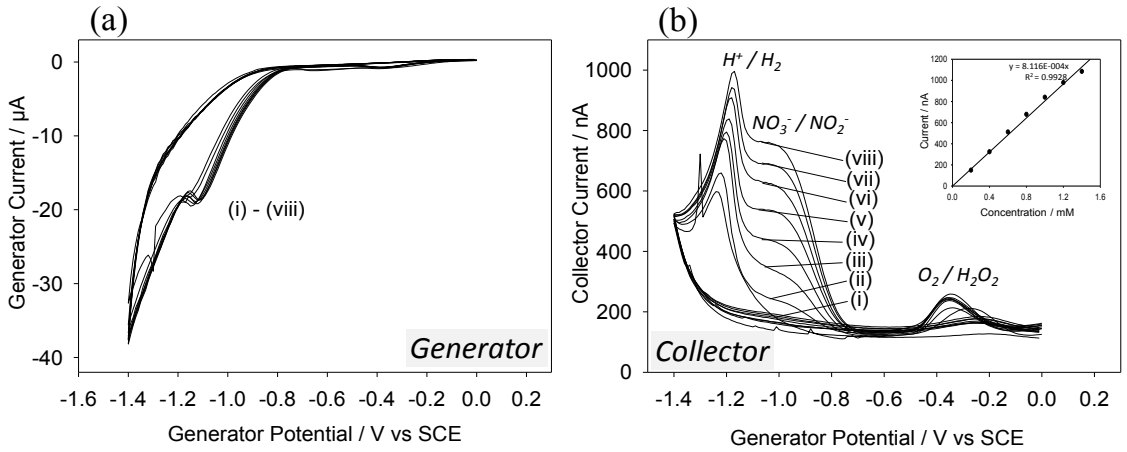

Figure 6

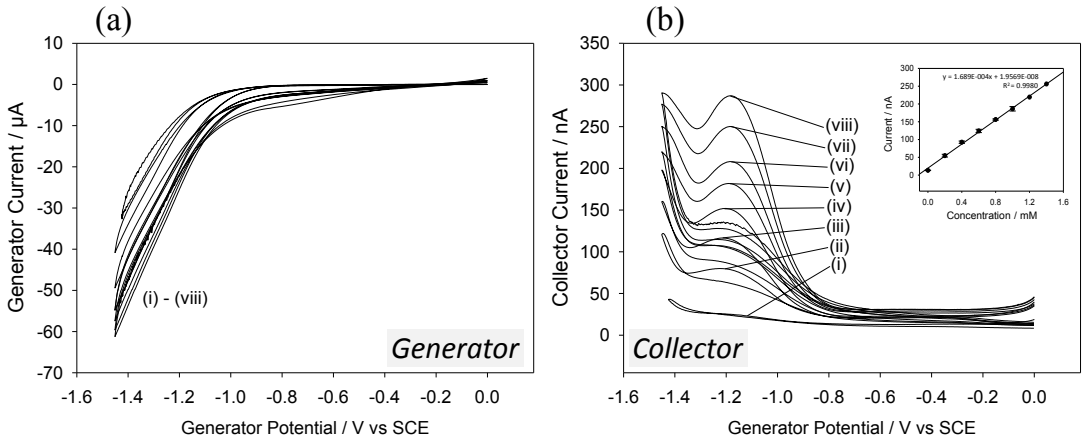

Figure 7